Pacific Northwest
NATIONAL LABORATORY

PNNL-32033

Speciation Correlations between Uranium and Iodine

September 2021

James M Bowen
Leah M Arrigo
Matthew A RisenHuber
Nicolas E Uhnak
Bethany M Lawler
Caleb J Allen
Andrew M Ritzmann
Katie A Wagner

U.S. DEPARTMENT OF ENERGY

Prepared for the U.S. Department of Energy
under Contract DE-AC05-76RL01830

PACIFIC NORTHWEST NATIONAL LABORATORY
operated by
BATTELLE
for the
UNITED STATES DEPARTMENT OF ENERGY
under Contract DE-AC05-76RL01830

Printed in the United States of America

Available to DOE and DOE contractors from
the Office of Scientific and Technical Information,
P.O. Box 62, Oak Ridge, TN 37831-0062
www.osti.gov
ph: (865) 576-8401
fox: (865) 576-5728
email: reports@osti.gov

Available to the public from the National Technical Information Service
5301 Shawnee Rd., Alexandria, VA 22312
ph: (800) 553-NTIS (6847)
or (703) 605-6000
email: info@ntis.gov
Online ordering: http://www.ntis.gov

PNNL-32033

Speciation Correlations between Uranium and Iodine

September 2021

James M Bowen
Leah M Arrigo
Matthew A RisenHuber
Nicolas E Uhnak
Bethany M Lawler
Caleb J Allen
Andrew M Ritzmann
Katie A Wagner

Prepared for
the U.S. Department of Energy
under Contract DE-AC05-76RL01830

Pacific Northwest National Laboratory
Richland, Washington 99354

Summary

The National Nuclear Security Administration’s Office of Conversion has been supporting development of molybdenum-99 production methods utilizing non-highly enriched uranium targets. One of the novel methods being considered is the use of an aqueous homogeneous subcritical system. Concerns about controlling potentially volatile radioiodine have led to efforts to characterize the iodine species in this system. This report examines the potential to characterize the chemical species of the iodine by correlating it with analyses of uranium, which is more abundant in the target material and suitable for on-line monitoring. Uranium quantification is viable in complex solutions with the use of chemometric modeling utilizing spectral analyses. Direct measurement of the iodine species would be infeasible due to the difficulty in performing analyses. Due to the complex nature of iodine chemistry and the stability of the uranyl species, there does not appear to be any correlation between the uranium and iodine species.

Acronyms and Abbreviations

cm	centimeter(s)
CNMR	carbon nuclear magnetic resonance
CSSWV	cathodic stripping square wave voltammetry
e^-_{aq}	solvated electron
EM	electromagnetic
ESR	electron spin resonance
H^1NMR	proton nuclear magnetic resonance
ICP-MS	inductively coupled plasma mass spectrometry
IR	infrared
ISE	iodine sensitive electrode(s)
keV	kilo-electron volt
K_{sp}	solubility product constant
LET	linear energy transfer
NIR	near infrared
nm	nanometer(s)
nM	nanomolar
PNNL	Pacific Northwest National Laboratory
ppb	parts per billion
ppm	parts per million
S-K	Sandell-Kolthoff
TBP	tributylphosphate
µm	micrometer(s)
µM	micromolar
UREX	uranium extraction
UV-Vis	ultraviolet-visible
V	Volt
XANES	X-ray absorption near-edge structure

Contents

Figures

Tables

1.0 Introduction

The National Nuclear Security Administration's (NNSA's) Office of Conversion (NA-231) has been focused on production of molybdenum-99 (Mo-99) using low enriched uranium (LEU) instead of highly enriched uranium (HEU). A new approach to meeting the demand for this crucial diagnostic medical isotope is the use of an aqueous homogenous subcritical system which has the benefit of the target material already being solution thereby avoiding the need to dissolve the irradiated target. However, the aqueous nature of the material allows for fission gases, such as radioxenon, to evolve. Depending on the conditions of the system, fission product iodine, or radioiodine – the precursor to xenon, may evolve as well.

Controlling radioiodine, particularly throughout an aqueous system, is important for protecting worker safety, the environment, and public health. Iodine's multiple oxidation states and potential for volatility present many challenges for controlling the fission product and necessitate characterization for a given system. The relatively low concentration of iodine in a solution of bulk uranium and other potential interferences presents challenges to direct determination of the chemical form of the iodine and, subsequently, managing the iodine inventory appropriately. If there was a correlation to another analyte, such as uranium, then characterization and control of the radioiodine could be more effective. An ideal characterization technique would include on-line monitoring of the uranium to track chemical changes to the iodine inventory and could be used to monitor system conditions.

This report examines potential signatures of uranium that can be exploited to characterize and monitor the chemical species of iodine in an aqueous homogeneous subcritical system. While the emphasis is on a sulfate matrix, a general review is discussed. The techniques described to analyze uranium focus on on-line monitoring. Techniques describing iodine signatures and characterization are broader and highlight their ineffectiveness in on-line monitoring. An overview of the reduction-oxidation (redox) chemistry for each element is included.

2.0 Potential Chemical Signatures

Spectroscopic analysis methods can be used for quantitative analysis through the interaction of an analyte of interest with electromagnetic (EM) radiation. When EM radiation is absorbed by an analyte, it may be possible to quantify using ultraviolet-visible (UV-Vis) and/or infrared (IR) spectroscopies. When EM radiation is scattered, it may be possible to quantify using Raman spectroscopy (Skoog et al. 1998). Other types of interactions with EM radiation are possible but UV-Vis, IR, and Raman will be the primary focus for uranium analysis because they can be implemented in remote and/or on-line measurements through technology such as fiber optic cables.

UV-Vis absorption and emission spectroscopy involves the excitation of bonding electrons and is applicable in the 180-780 nm range (1.3×10^4-5×10^4-cm^{-1} wavenumber). IR and Raman spectroscopies involve the rotation and/or vibration of molecules and are applicable in the 0.78-300 µm range (3.3×10^1-1.3×10^4 cm^{-1} wavenumber). IR and Raman are complementary techniques with Raman having the benefit that water is not Raman active while it is IR active (Skoog et al. 1998).

Spectroscopic analysis techniques like UV-Vis, IR, and Raman can be applied to the simultaneous measurement of multiple analytes in remote and/or on-line measurements. These techniques can be implemented in a relatively simple setup and the use of multiple techniques permits measurements across a broad portion of the electromagnetic spectrum. Under ideal conditions, absorbance measurements can be used to quantify an analyte with Beer's law using the equation $A = abc$. Beer's law states that for monochromatic radiation the absorbance (A) is directly proportional to the path length (b) through the medium and the concentration (c) of the absorbing species where the absorptivity (a) is a proportionality constant (Skoog et al. 1998).

The use of spectroscopic techniques does have limitations. Solution conditions and/or a complex matrix have the potential to impact the spectral signature of some analytes with the sensitivity to changes in the spectra being analyte dependent. Changes to the spectral signatures can include strong baseline shifts, changes in spectral peak shape, and overlapping bands which all limit the direct application of Beer's law. Additionally, accurate characterization can be negatively impacted by interference from other species present in complex matrices, dynamic solution conditions such as solution temperature and the presence of solids in a flow condition setup, as well as the presence of an intense radiation field (Tse et al. 2020).

Accurate quantification of complex solutions can be achieved even in solutions with analytes having spectral interferences using chemometric analysis. This method applies mathematical and statistical methods to the simultaneous analysis of multiple wavelengths/wavenumbers (Tse et al. 2020). Kirsanov et. al. (2017) provided a review of chemometric analysis of UV-Vis spectra showing that while basic UV-Vis analysis suffers from low selectivity, the use of chemometrics allows for accurate quantification of multiple analytes in complex solutions for multiple applications.

Other analytical methods, such as mass spectrometry, can provide improved detection limits, but are often destructive, may require chemistry to prepare samples, or not conducive to on-line monitoring. A brief review of additional techniques is presented below in a discussion of iodine analytical techniques.

2.1 Uranium Chemical Signatures

2.1.1 Actinide oxidation states and speciation

The middle actinides, including U, Np, Pu, and Am, display complex solution chemistry and can be present in a variety of oxidation states and complexes. As shown in Table 1, each element can attain 4-5 oxidation states and a solution may contain more than one oxidation state of an element at the same time. The oxidation states and complexes present in a solution are dependent variables such as analyte concentration, matrix, presence of complexing ions and/or redox agents, temperature, as well as kinetics moving between the oxidation states (Greenwood and Earnshaw 1997).

In aqueous solutions, oxidation state VI is dominated by the actinyl ion MO_2^{2+}. The M-O bond strength and resistance to reduction decreases in the order of U > Np > Pu > Am; in aqueous solutions, U is typically present as UO_2^{2+} unless a relatively strong reducing agent is added. The MO_2^{2+} ion is highly charged making it is possible for the MO_2^{2+} ion to undergo hydrolysis which results in polymerization and -OH- bridges and species such as $[(UO_2)(OH)]^+$, $[(UO_2)_2(OH)_2]^{2+}$, $[(UO_2)_3(OH)_5]^+$. Hydrolysis can be minimized or prevented by the addition of stabilizing complexing ions, redox agents, etc. (Greenwood and Earnshaw 1997).

Table 1. Actinide Oxidation States (Greenwood and Earnshaw 1997).

Species present in H_2O	U	Np	Pu	Am
M^{3+}	3	3	3	**3***
M^{4+}	4	4	**4***	4
MO_2^+	5	**5***	5	5
MO_2^{2+}	**6***	6	6	6
MO_5^{3-}	------	7	7	------
*Most stable oxidation state in aqueous solution				

The most stable oxidation state for Np is V which is the dominant species present as NpO_2^+ in aqueous solutions or extracts from aqueous solutions. The equilibria between the IV, V, and VI oxidation states are complex and dependent on a variety of factors including the solution composition, temperature, etc. Neptunium (V) is also known to form coordination complexes with anions as well as cation-cation complexes such as $NpO_2^{+}{*}UO_2^{2+}$. The characteristic NpO_2^+ band at 981 nm in the visible-near IR (Vis-NIR) spectrum, observed in 1 M HNO_3 solutions, can be split into two bands when UO_2^{2+} is present (Arrigo et al. 2009).

2.1.2 Spectroscopic-chemometric analysis

UV-Vis, IR, and Raman spectroscopy have all been demonstrated in the measurement of a wide variety of analytes including actinides, lanthanides, transition metals, and various inorganic and organic ions (i.e., nitrate, oxalate, etc.) providing applicable baseline signatures. As discussed by Tse et al. (2020), spectroscopic-chemometric based analysis has been applied to the accurate quantification of actinide, lanthanide, acid, and polyoxo-anions as well as monitoring actinide speciation in real time for on-line and near-real-time processing of nuclear materials including nuclear fuel reprocessing and legacy waste management. Processing nuclear materials involves monitoring a complex matrix in a high radiation field with limited access to the material being processed. Such materials include a wide variety of analytes of interest but also potential interferences. Primary components of the starting material include irradiated U and the nitrate matrix along with a variety of fission products and other actinides such as Np, Pu, and Am present from material irradiation, transition metals such as Hg, Fe, and Cr present from storage containers and process equipment and/or potentially added for subsequent chemical separations, as well as a variety of inorganic and organic ions such as oxalate which may have been added during material storage and/or added for subsequent chemical separations. Use of spectroscopic-chemometric analysis must consider all chemical constituents as potential spectral interferences and/or as potential redox agents which may alter the oxidation state of the metal analyte of interest therefore altering the spectral signature.

Chemometrics is, fundamentally, the application of a multivariate chemical model to a data set for the purposes of extracting the greatest amount of information (Wold 1995). The model, trained from a controlled set of experiments, provides the means for inverting complex spectra into concentrations of individual species. Tse et al. (2020) also discuss several limitations to spectroscopic-chemometric analysis for nuclear material processing including development of customized models, the acquisition of basic and accurate information for testing the models, and the limited techniques utilized in building current models. Models used in the current nuclear material processing research may not be suitable for increasingly complex processing streams necessitating development of more sophisticated models. The models then require basic and accurate information from test samples to ensure accuracy; however, obtaining these test samples can be difficult due to radiological dose rates, cost, and access limitations. Models are also limited by the techniques used in the chemometric analysis and the inclusion of additional techniques such as physiochemical measurements allows for development of increasingly sophisticated models; however, as with obtaining a test sample, obtaining data for additional techniques (i.e., gamma energy analysis, density, conductivity, pH, etc.) can be difficult. As discussed by Tse et al. (2020) models incorporating both spectroscopic and physiochemical measurements can be biased toward the spectroscopic measurement due to the large number of variables included in the measurement. This bias can be minimized by using principal component analysis to minimize the spectroscopic data set. The different techniques can then contribute more equally to the model since less relevant information has been removed from the complex spectroscopic data sets (Tse et al. 2020).

Obtaining analytical results from spectroscopic-chemometric analysis of complex samples requires appropriate models which address the various constituents which may be present in the sample as well as the experimental conditions such as temperature, analyte concentrations, etc. The models can be customized for the system of interest allowing for the most accurate and precise results possible; the models become more accurate as the number of training experiments and physicochemical techniques included increases.

2.1.3 UV-Vis, Raman, and IR Analyses

UV-Vis, Raman, and IR bands for select analytes of interest are shown in Table 2 and Table 3. The bands for the uranyl sulfate system given in Table 3 are also presented by Gal et al. 1992 in addition to a spectrum and the deconvolution into the component peaks; the spectrum is quite complex even for a two-component system in water, but it is possible to deconvolute the various peaks knowing the stretches which are IR active for sulfate and uranyl ions. Figure 1 shows an example of the use of spectral deconvolution on the relatively complex spectra of Ce complexed to the dye Arsenazo III, data collected at PNNL as reported in PNNL-28366. In more complex solutions such as nuclear material processing which includes a wide array of components including the matrix, uranyl, actinides formed during irradiation, fission products, various anions from processing, etc. such a method would not be able to resolve the various peaks to determine metal complex species, oxidation states, and/or metal concentrations. The use of spectroscopic-chemometric analysis can use more sophisticated customized models to perform the deconvolution.

Table 2. Raman and UV-Vis Bands for Select Analytes of Interest.

	Raman (cm^{-1})	UV-Vis-NIR (nm)	References
UO_2^{2+}	870		Arrigo et al. 2009; Burneau and Tazi 1992
$UO_2(SO_4)$	861		Burneau and Tazi 1992
$UO_2(SO_4)_2^{2-}$	852		Burneau and Tazi 1992
$UO_2(SO_4)_3^{4-}$	843		Burneau and Tazi 1992
NpO_2^+		981*	Arrigo et al. 2009
NpO_2^{2+}		1220	Arrigo et al. 2009
Pu^{4+}		657, 851, 701, 792	Arrigo et al. 2009
NO_3^-	1047		Arrigo et al. 2009; Burneau and Tazi 1992
SO_4^{2-}	981		Burneau and Tazi 1992
HSO_4^-	1048		Burneau and Tazi 1992

*This band can be split in the presence of UO_2^{2+} due to formation of cation-cation complexes [Arrigo et al. 2009].

Table 3. Infrared and Raman Bands of Uranyl and Sulfate Complexes in Aqueous Solutions (Gal et al. 1992).

HSO_4^-	**Na_2SO_4**	**UO_2SO_4***	**$Na_2UO_2SO_4$***	**$Na_4UO_2(SO_4)_3$***		**Assignment**
IR (cm^{-1})	IR (cm^{-1})	IR (cm^{-1})	IR (cm^{-1})	IR (cm^{-1})	Raman (cm^{-1})	
1200		1184 sh	1186 sh	1189 sh		$\nu_3(SO_4)$
		1144 vs	1138 vs	1133 vs	1174 w	$\nu_3(SO_4)$
					1130 vw	
	1103 vs	1144-1047 – Free SO_4^{2-} is not present but could be contributing to the overlap region				$\nu_3(SO_4)$
1051		1047 s	1044 vs	1043 s	1045 w	$\nu_3(SO_4)$
					1037 w	
	980 vw **	956 s	963 s	967 m	983 s	$\nu_4(SO_4)$, UO_2 asym str
			950 sh	945 sh	950 m	UO_2 asym str
		900 w,b		888 sh		
		860 w	855 vw	853 vw	963 vs	UO_2 sym str
		650 sh				
	611 w	610 vw				$\nu_4(SO_4)$
		595 vw				
		259 vs				UO_2 bending
		208 w,b				U-O ligand str

s – strong, vs – very strong, m – medium, w – weak, vw – very weak, sh – shoulder, b – broad, str - stretch

*UO_2SO_4 – 0.5 M; $Na_2UO_2SO_4$ – 1 mL 1 M UO_2SO_4 + 1 mL 1 M Na_2SO_4; $Na_4UO_2(SO_4)_3$ – 1 mL 0.5 M UO_2SO_4 + 1 mL 0.5 M Na_2SO_4

** Indicates distorting interaction with the solvent

It is possible to use spectroscopic-chemometric analysis to quantify analytes through their effect on other analytes. The concentrations of UO_2^{2+} and HNO_3 can be quantified simultaneously; however, direct quantification of HNO_3 has a high relative error due to a lack of a distinguishable band in the visible region. The HNO_3 concentration can instead be quantified based on the subtle effect nitrate has on the UO_2^{2+} spectra due to formation of uranyl-nitrate complexes (Tse et al. 2020). Analyses performed by Gal et al. show the stoichiometry of the uranyl sulfate species can be determined through subtle changes to the IR and/or Raman bands for both uranyl and sulfate, see Table 3 (Gal et al. 1992).

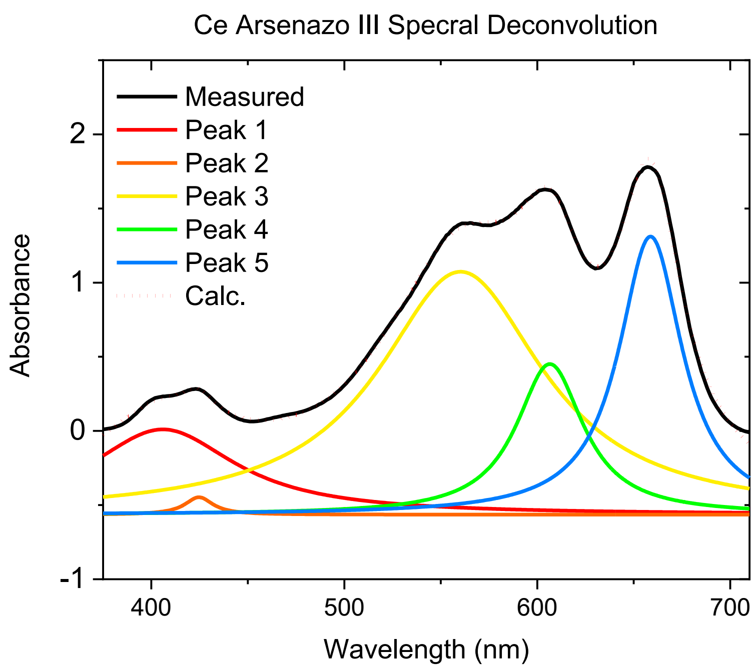

Figure 1. Spectral deconvolution of 25 ppm Ce(III) in 1×10^{-4} M Arsenazo III, 0.5 M ammonium citrate, at pH 4. Fitting process used Lorentzian function, fitting the five visible peaks to these functions. The calculated sum of the fitted peaks is shown as the dotted red line.

2.2 Iodine Chemical Signatures

This section discusses the identification of iodine compounds using Raman, UV-Vis, IR, and other analytical techniques, where appropriate. There are several iodine complexes and ions that may be formed in freshly irradiated nuclear fuel, including the following:

- Iodide (I^-) and iodate (IO_3^-) are some of iodine's more stable ions.
- Molecular iodine (I_2) is a volatile species which can exist in solution though it may disproportionate into hypoiodous acid (HIO) and hydroiodic acid (HI). Acidic conditions stabilize I_2 by inhibiting the disproportionation reaction (Carter 1925).
- Methyl iodide (CH_3I), also known as iodomethane, can form whenever iodine/iodide is in contact with organics (Keilholtz and Barton 1965).

- Triiodide (I_3^-) is formed only when higher concentrations of I_2 are present as it typically exists as I_2 and I^- chains (Svensson and Kloo 2003; Alvarez et al. 2010). These polyiodide chains can also form I_4^{2-}, I_5^-, and at times I_7^- (Kaiho 2015).

- Hypoiodous acid (HIO) and hypoiodate (IO^-) are typically considered to be intermediates for reactions causing I_2 to form IO_3^- and IO_3^- to form I_2 in irradiated nuclear fuel (Bray and Liebhafsky 1931; Liebhafsky 1932; Liebhafsky 1931; Liebhafsky 1934; Liebhafsky and Wu 1974; Liebhafsky et al. 1978; Liebhafsky et al. 1981).

- Iodic halogens (IX_N) can be formed when iodine complexes with other halogens, and these can range up to at least an additional seven atoms. These complexes will form if halogens are present in appreciable concentrations in the nuclear fuel during irradiation (Kaiho 2015).

- Periodate (IO_4^-) is a form of iodine which can exist in several different forms from IO_4^- to $H_5IO_6^-$ and typically requires strong oxidizing and acidic conditions (Crouthamel et al. 1949).

- Pentathionate iodide ($S_5O_6I^-$): formation may occur when concentrations of at least 63 mM iodine were present (Xu et al. 2012) although the literature on this compound is limited.

- Solid iodides can be present in freshly irradiated nuclear fuel, including silver iodide (AgI), copper (I) iodide (CuI), lead (II) iodide (PbI_2), and palladium (II) iodide (PdI_2). AgI has been considered one of the most stable waste forms for iodine radioactive waste, despite being sensitive to light (Kaiho 2015). CuI is formed following the reduction of Cu^{2+} to Cu^+ through reaction with iodine (Kaiho 2015). PdI_2 is quite stable with a solubility product of PdI_2 is 7×10^{-32} M^3 (Elding and Olsson 1986).

2.2.1 Iodine Compound Identification using Raman

Triiodide, iodide, and iodate can be identified using Raman; Table 4 includes a compilation of results from spectroscopic techniques for iodine, iodide, and iodate.

- Iodide can be observed when it is paired with an indicator, such as cuprite (Cu_2O), but is not detected by itself until at a high enough concentration to produce polyiodides (Lefèvre et al. 2000).

- Iodide can be quantified using starch-reduced gold nanoparticles and the appearance of a peak at 2125 cm^{-1}; this technique can detect iodine in the range of 0.01 – 2.0 µM (Pienpinijtham et al. 2011).

- Iodate is detected near 800 cm^{-1} when in the aqueous phase and near 775 cm^{-1} as a solid paired with an alkali metal (Gardiner et al. 1972; Dasent and Waddington 1960).

- There are multiple forms of I_3^- and I_5^- and each have a different Raman frequency (Kaiho 2015).

- Polyiodides have also been observed (Alvarez et al. 2010).

Table 4. Raman and UV-Vis Bands for Select Iodine Analytes of Interest.

Iodine Species	Raman (cm^{-1})	UV-Vis (nm)	Reference(s)
Iodine	174	525	Semnami et al. 1996; Kaiho 2015; Lefevre et al. 2000
Symmetric I_3^- $(I\text{-}I\text{-}I)^-$	110 s	285 and 355	Kaiho 2015; Kireev and Shnyrev 2015
Asymmetric I_3^- $(I_2 \cdot I^-)$	167 s, 143 w, 114 w		Kaiho 2015
I_5^- linear $(I_2 \cdot I\text{-} \cdot I_2)$	160 s, 104 w		Kaiho 2015
I_5^- V shaped $(I_2 \cdot I^- \cdot I_2)$	167 s, 131 m, 114 w		Kaiho 2015
I_5^- L shaped $(I_3^- \cdot I_2)$	164 s, 135 m, 106 w		Kaiho 2015
Iodide	*	180-220	Kireev and Shnyrev 2015; Dasent and Waddington 1960; Van Stipdonk et al. 2000
Iodate	800 (aqueous)	180-220	Kireev and Shnyrev 2015; Dasent and Waddington 1960; Gardiner et al. 1972; Van Stipdonk et al. 2000
Pentathionate Iodide		468	Xu et al. 2012

m = medium, s = strong, w = weak

* Iodide is visible when high concentrations as polyiodides in multiple bands such as 110, 167, and 114 cm^{-1}.

2.2.2 Iodine Compound Identification using UV-Vis

Various iodine species can be identified and potentially quantified using UV-Vis if sufficient amounts of the species is present. Iodine is produced is low quantities by mass during fission and quantification using UV-Vis is not typically feasible.

- Iodine is visible at 525 nm (Semnami et al. 1996).

- Iodide and iodate absorb in the 180-220 nm range although they typically aren't distinguishable even at millimolar concentrations when using UV-Vis spectroscopy (Kireev and Shnyrev 2015).

- Triiodide produces two maxima at 285 and 355 nm (Kireev and Shnyrev 2015).

- Pentathionate iodide is visible at 468 nm using UV-Vis, however, UO_2^{2+} interferes at this wavelength (Xu et al. 2012).

- None of the solid iodides (AgI, CuI, PbI_2, PdI_2) will be formed in large amounts due to low fission yields of these metal ions and none of them will be observable via UV-Vis or other forms of liquid analysis.

2.2.3 Iodine Compound Identification using IR

Iodine itself cannot be identified via IR spectroscopy. There are however some iodine containing compounds that can. Periodate can be observed via IR around 856 cm^{-1} (11.68 μm) (Al-Kayssi 1963). Silver iodide has an IR band near 195 cm^{-1}.

2.2.4 Iodine Compound Identification using Other Analytical Techniques

There are a variety of other analytical techniques that can be used to identify iodine compounds; some of these techniques, their applications, detection limits, etc. are given in Table 5.

Table 5. Additional analytical techniques for analysis of iodine compounds

	Technique*	Additional Information	References
I_2	XANES	>0.2 mg/L iodine	Shelor and Dasgupta 2011
I^-	ISE	>20 μM	Shelor and Dasgupta 2011
I^-, IO_3^-	Titration Sandell-Kolthoff (S-K)	reaction (a titration of Ce^{4+} to Ce^{3+} via As, catalyzed by I^-)	Kaiho 2015
I^-, IO_3^-	CSSWV**	Sea water, >20 nM	Wong and Zhang 1992;
IO_3^-	CSSWV** with Differential pulse polarography		Cook et al. 2000
I_2, I^-, IO_3^-, complexes	ICP-MS	Typically >0.1 ppb iodine	Yoshida et al. 2007; Leiterer et al. 2001; Zheng et al. 2011; Shelor and Dasgupta 2011
CH_3I	H^1NMR, CNMR, IR, ESR	H^1NMR: 2.162 ppm CNMR: -23.59 ppm	National Institute of Advanced Industrial Science and Technology 2018
U	CSSWV** CSSWV**	Trace levels U in molten salts up to 1.7% by weight	van Elteren et al. 1995 Iizuka (2001)

*CSSWV - cathodic stripping square wave voltammetry
*ISE - ion sensitive electrodes
*XANES - K-edge X-ray absorption near-edge structure; requires a beamline
** CSSWV is typically used for trace analysis and may not be reproducible in complex matrices. A complex matrix of bulk uranium and other potential interferences could affect the viability of this method.

3.0 Reduction-Oxidation Chemistry

Chemistry is affected by the reduction and oxidation of a compound's oxidation state, particularly in a complex solution. These reduction-oxidation (redox) reactions are often driven by one compound's ability to reduce, as a reducing agent, or increase, as an oxidizing agent, the oxidation state of another compound. The presence of ionizing radiation can further affect redox chemistry through the creation of intermediates and catalysts by a process called radiolysis.

3.1 Radiolysis

Radiolysis can be significant contributor to the solution chemistry, particularly under prolonged irradiation whether that be neutron irradiation or other sources of radiation such as alpha, gamma, or electrons (beta decay equivalent). This section focuses on the effects of radiolysis on solutions, focusing on sulfate media but will include discussions related to the uranium extraction (UREX) separation scheme and similar systems. The effects on the "target", the molecule, surface etc. that receives the energy from the radiation is dependent on the energy of the radiation as well as the LET (linear energy transfer) of that radiation, an alpha particle has a high LET meaning it deposits the bulk of its energy in the first few collisions (Choppin et al. 2002).

3.1.1 Radiolysis of Aqueous Solutions

In an aqueous solution, water is the primary target of radiolytic degradation. Figure 2 shows the basic gamma radiolysis products from the irradiation of water and the time scales associated with those reactions. There are radicals, gases, acids bases and solvated electrons produced through radiolysis. Each of those products can then act in their own capacity with other solution constituents. These reactions are called spur reactions. These spur reaction products are included in Table 6 (Choppin et al. 2002).

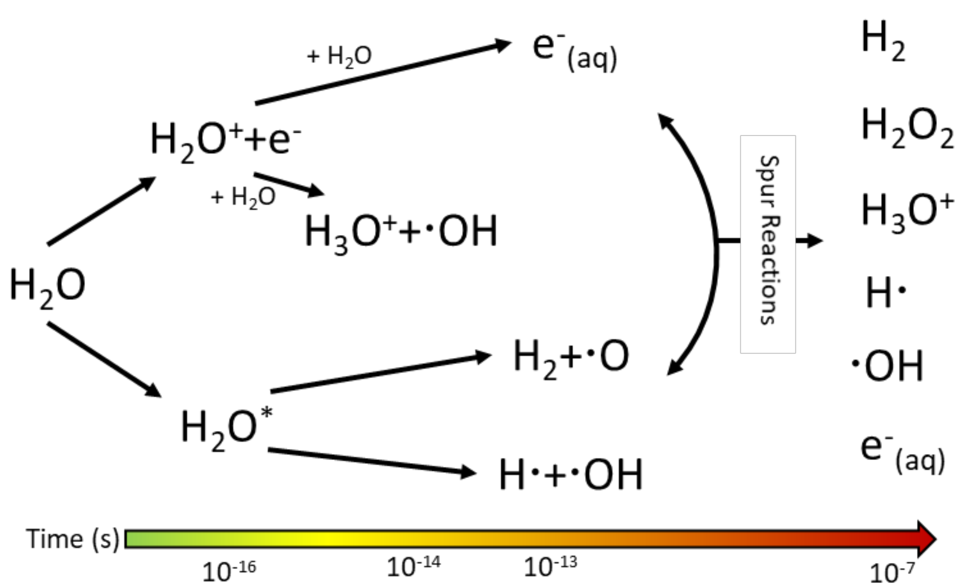

Figure 2. Gamma radiolysis of water. Adapted from Lousada et al. 2016 and Choppin et al. 2002.

Table 6. Water radiolysis spur reaction products from Choppin et al. 2002.

$e_{aq}^- + e_{aq}^- + 2H_2O \rightarrow H_2 + 2OH^-$
$e_{aq}^- + \bullet OH \rightarrow OH^-$
$e_{aq}^- + H^+ \rightarrow \bullet H$
$e_{aq}^- + \bullet H + H_2O \rightarrow OH^- + H_2$
$\bullet H + \bullet H \rightarrow H_2$
$\bullet OH + \bullet OH \rightarrow H_2O_2$
$\bullet OH + \bullet H \rightarrow H_2O$
$OH^- + H^+ \rightarrow H_2O$

The radiation's LET controls the formation of many of these transient water radiolysis products. Table 7 shows the effects of the LET on the formation of radiolysis products. In this table, the G-value is used, which is the number of molecules produced per unit energy absorbed. As the LET increases, in the case of the 12 MeV alpha, the probability of forming molecular species such as H_2O_2 increases.

Table 7. Product Yields, G-values, (μmol/J) in Irradiated Water from Choppin et al. 2002.

Radiation	G (-H_2O)	G(H_2)	G(H_2O_2)	G(e^-_{aq})	G(H·)	G(·OH)	G(·HO_2)
γ	0.43	0.047	0.073	0.28	0.062	0.28	0.0027
12 MeV α	0.294	0.115	0.112	0.0044	0.028	0.056	0.007

Many of these radiolysis products are maintained in solution, including sulfuric acid or sulfate containing solutions. A number of these reactions are pH dependent, for instance solvated electron (e^-_{aq}) is highly pH dependent and is effectively non-existent in acidic solution in an appreciable time frame (Choppin et al. 2002). Some of solutes act as scavengers, removing some of these from consideration. In a 0.4 M sulfuric acid solution there is a slight hindrance of the formation of molecular species as a function of the radiation's LET. This is likely due to the reactant species, such as •OH, being consumed in sulfate reactions like those shown in Table 8.

Table 8. Table of Sulfate Radiolysis Products obtained from Jiang et al. 1992.

Reaction	k/dm^{3}mol^{-1}s^{-1}
$OH + HSO_4^- \rightarrow SO_4^- + H_2O$	k_3
$OH + H_2SO_4 \rightarrow SO_4^- + H_3O^+$	k_4
$H + S_2O_8^{2-} \rightarrow SO_4^- + HSO_4^-$	2.5×10^7
$H + HSO_3^- \rightarrow SO_4^- + H_2O$	2.2×10^8
$H + SO_4^- \rightarrow HSO_4^-$	1.0×10^{10}
$SO_4^- + SO_4^- \rightarrow S_2SO_8^{2-}$	7.6×10^8
$SO_4^- + H_2O_2 \rightarrow HSO_4^- + HO_2$	1.2×10^7
$SO_4^- + HO_2 \rightarrow HSO_4^- + O_2$	3.5×10^9
$SO_4^- + OH \rightarrow HSO_5^-$	1×10^9
$SO_4^- + S_2O_8^{2-} \rightarrow SO_4^{2-} + S_2O_8^-$	6.6×10^5
$SO_4^- + H_2O \rightarrow HSO_4^- + OH$	500 s^{-1}

Radiolysis products are responsible for potential sources of redox activity, for example in the radiolysis products of sulfate is the production of persulfate ions, a powerful oxidizing agent with a reduction potential of 2.1 V (CRC Handbook of Chemistry and Physics 2009). The production of persulfate, peroxides, and solvated electrons provide sources of redox adjustments of other solution constituents.

Iodine is affected by many of these radiolysis products, largely through redox mechanisms. Many of the literature investigations do not use fission solutions, largely due to the low concentrations of iodine in fission samples relative to those required for speciation determination. Sawai et al. (1966) discusses iodine under aqueous radiolysis conditions, namely as a solution of KI under ^{60}Co irradiation, as well as the role of pH finding that there is an inverse relationship between the G-values for the formation of I_2 and H_2O_2. Above trace level concentrations, I_2 readily forms in acidic conditions without the aid of radiolysis. The primary mode of decay in a fission sample is the beta decay from the fission products, these beta decays subsequently produce short lived intermediate solvated electrons that can promote radiolysis and are highly pH dependent. The interaction between radiolysis products and iodine are included in Table 9. Included in this table are short-lived intermediate or transient species that may not exist for extended periods of time. Many of these products, iodine or otherwise are pH dependent.

Table 9. Interaction Between Radiolysis Products and Iodine taken from Sawai et al. 1966.

$2I^- + H_2O_2 + 2H^+ \rightarrow 2I + 2H_2O$
$I + I \rightarrow I_2$
$I + I^- \rightarrow I_2^-$
$I_2^- + I_2^- \rightarrow I_3^- + I^-$
$I_2 + I^- \leftrightarrow I_3^-$
$e_{aq}^- + I \rightarrow I^-$
$e_{aq}^- + H^+ \rightarrow H + I^- + H^+ \rightarrow H_2 + I$
$H + I \rightarrow H^+ + I^-$
$O_2^- + I \rightarrow O_2 + I^-$
$HO_2 + I^- + H^+ \rightarrow H_2O_2 + I$
$I_2^- + H_2O_2 \rightarrow 2I^- + H^+ + HO_2$
$I_3^- + H_2O_2 \rightarrow 3I^- + 2H^+ + O_2$
$I_2 + HO_2 + I_2^- + H^+ + O_2$
$I_2^- + HO_2 \rightarrow 2I^- + H^+ + O_2$

3.1.2 Radiolysis of Extraction Solvent

An example of how radiolysis can impact iodine chemistry is demonstrated by radiolytic effects of solvent extraction of irradiated material. Tributylphosphate (TBP) has widespread usage for the separation of irradiated uranium and a wealth of knowledge on the radiolysis of TBP has been generated (Choppin et al. 2002; Mincher et al. 2009). One of the primary efforts have been focused on the understanding and characterization of the so-called “Red Oil”, an unstable explosive oil that forms from the radiolysis of the 30% TBP extraction solvent used in UREX or UREX-like extractions (Srinivasan and Vasudeva Rao 2014). The primary decay products of TBP are shown below in Figure 3, there are multiple pathways to obtain the same product in this case the dibutyl hydrogen phosphate, HDBP, including many involving radicals stemming from water, extracted nitric acid, from another TBP molecule or fragment, as well as the diluent, such as dodecane, see Table 10 for examples of radical formation on TBP (Mincher, et al. 2009; Mincher et al. 2008). The further degradation of the HDBP will occur sequentially until there is phosphoric acid and butene (Mincher et al. 2009; Pearson and Nilsson 2014). Production of these TBP radiolysis products decreases with the number of cleaved butyl groups (HDBP>H_2BP>Phosphoric acid) (Mincher et al. 2009; Pearson and Nilsson 2014).

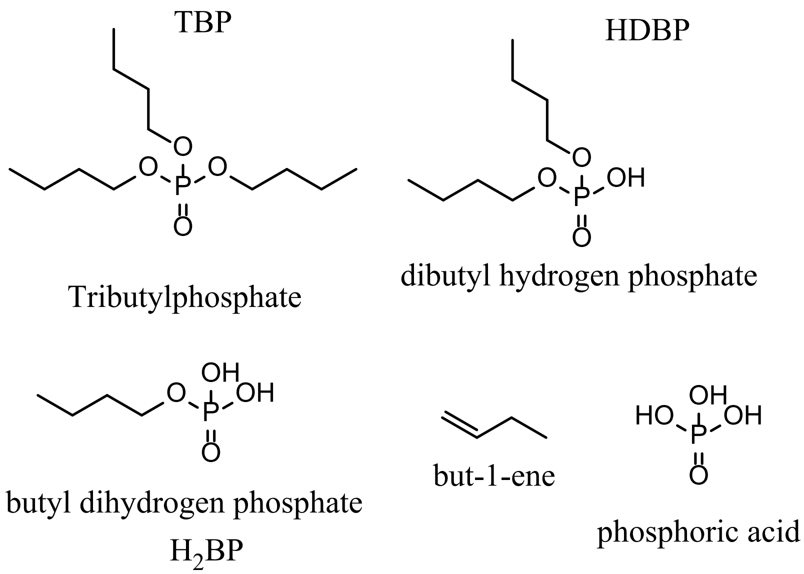

Figure 3. Primary Radiolytic Products of TBP under Radiation (Mincher et al. 2009).

Table 10. Examples of Radical Formation Involving TBP (Mincher, et al. 2009; Mincher et al. 2008).

$(\bullet\, C_4H_8O)(C_4H_9O)_2PO \rightarrow (C_4H_9O)_2OPO^- + \bullet\, C_4H_8$
$\bullet\, H \ + TBP \rightarrow \ (\bullet\, C_4H_8O)(C_4H_9O)_2PO + H_2$
$\bullet\, OH \ + TBP \rightarrow \ (C_4H_9O)_2(\bullet\, C_4H_8O)PO + H_2O$

Unless scrubbed from solution these TBP radiolysis products persist in the extraction solvent, altering the extraction behavior, to be clear there needs to be a significant quantity of these products to cause significant issues.

The radiolytic degradation of TBP is impacted by the presence of iodine in solution (Nowak and Nowak 1986). In general, there is a slight retardation in the radiolysis of TBP when I^- is present, though this is also dependent on the HNO_3 concentration. This extraction system is also known to extract I_2, though other reactions are known to occur such as the formation of the I_3^- species in solution (Nowak and Nowak 1986; Sakurai, et al. 1995). Iodine is readily extracted by 30% TBP extraction solvents, producing a third phase in some cases for solutions that had been irradiated heavily (Sakurai, et al. 1995). In solutions containing a significant quantity of iodine, the formation of organic iodides is promoted through interaction between the iodine and the organic degradation products from the extraction solvent (Nowak and Nowak 1986; Sakurai, et al. 1995).

3.2 Uranium Redox Chemistry

As discussed in Section 3.1, uranium can achieve oxidation states III, IV, V, and VI with IV and VI being stable in aqueous solutions. Uranium (VI) is present in aqueous solutions as the uranyl ion, UO_2^{2+}, which is highly stable. The uranium species and oxidation state can be impacted by the presence of radiolysis products such as peroxides, hydroxide radicals, persulfates, etc. The coordination environment for U is dependent on the species present as well as concentration; degradation of sulfate will alter the concentration which then impacts the number of coordinating sulfate ions. Kirsanov et al. (2017) showed that it is possible to monitor sulfate coordination with

UO_2^{2+} using UV-Vis and Gal et al. (1992) showed it is possible to monitor this parameter using IR and Raman. The uranyl ion coordination environment can be impacted by radiolysis products in solution such as peroxides and radicals to form hydrolysis products such as $[(UO_2)(OH)]^+$, $[(UO_2)_2(OH)_2]^{2+}$, $[(UO_2)_3(OH)_5]^+$ (Greenwood and Earnshaw 1997). With a sufficiently strong reducing agent, it is possible to reduce U(VI) to U(IV) with U(V) present as an intermediary species. The uranyl ion is highly stable and without a holding reductant is likely U(IV) will oxidize to U(VI); while U(IV) and U(V) may not be present at equilibria they may still be present as transient species which will impact on-line monitoring. Pourbaix diagrams for uranium in aqueous media highlight uranyl's stability, showing that across the entire pH range there are conditions for stable UO_2^{2+} to exist (Pourbaix 1974).

3.3 Iodine Redox Chemistry

According to Pearson's hard-soft acid-base theory, iodine is a soft base (Pearson 1963). It does not complex with uranyl ions (Prins et al. 1978). There are, however, some weak uranyl iodate complexes (Karbowiak et al. 2003). The strengths of these complexes are listed in Table 11.

Table 11. Thermodynamic constants for uranyl-iodate complexes where β_{11} and β_{12} are the stability constants for $UO_2(IO_3)^+$ and $UO_2(IO_3)_2$, respectively.

	Value	Method Obtained	Reference
$\log(\beta_{11})$	1.6 ± 0.1	Capillary Electrophoresis	Karbowiak et al. 2003
$\log(\beta_{11})$	1.5 ± 0.1	Fluorescence	Karbowiak et al. 2003
$\log(\beta_{12})$	3.05 ± 0.1	Capillary Electrophoresis	Karbowiak et al. 2003
$\log(\beta_{12})$	3.6 ± 0.2	Fluorescence	Karbowiak et al. 2003
$\Delta_f G_m°$ $UO_2IO_3^+$	-1090.3 ± 1.9 kJ/mol		Ragoussi et al. 2020
$\Delta_f H_m°$ $UO_2IO_3^+$	-1228.9 ± 1.8 kJ/mol		Ragoussi et al. 2020
$\Delta_f S_m°$ $UO_2IO_3^+$	91 ± 4.7 J/K*mol		Ragoussi et al. 2020
$\Delta_f G_m°$ $UO_2(IO_3)_2$	-1225.7 ± 2.5 kJ/mol		Ragoussi et al. 2020

Hydrolysis caused by fission will impact iodine speciation. If peroxides are produced, iodine, iodate, and iodide will react with them at differing rates depending on the acid concentration (Bray and Liebhafsky 1931). Peroxide will be catalytically consumed in the formation of iodine via iodate and iodate via iodine.

Complicating the chemistry in this system, iodine is well known for behaving differently depending on the solution potential (E_H) and its concentration (Pourbaix 1974). As shown in Figure 4, oxidizing conditions (high E_H) favor the formation of iodate while reducing conditions (low E_H) favor the formation of iodide. At high iodine concentrations (e.g., 1×10^{-3} moles per kg H_2O), the most stable species are I_2, I^- and IO_3^- depending on pH and E_H. At lower iodine concentrations (e.g., 1×10^{-7} moles per kg H_2O), I^+ has a region of stability in the low pH and moderately-high E_H region. At low concentrations relevant to this study, HOI/IO^- potentially become viable iodine species.

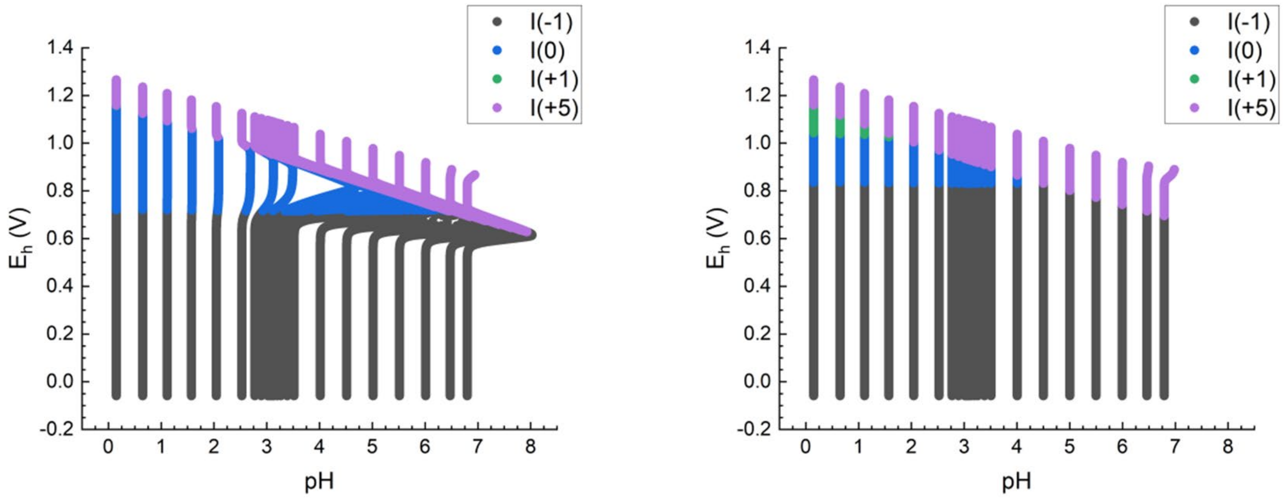

Figure 4. Potential – pH Equilibrium Diagram for the System Iodine-Water, at 25°C, for Solutions Containing 1×10^{-3} (left) and 1×10^{-7} (right) moles I per kg H_2O.

4.0 Conclusions

A review of analytical methods for uranium, primarily as the uranyl ion, and iodine characterization showed that on-line monitoring of uranium for an aqueous homogeneous subcritical system might be feasible, depending on the radiolytic effects of high radiation dose rates. However, direct characterization of the iodine species is more difficult and not suitable for on-line monitoring primarily due to concentration limits and the inability to identify the most stable iodine ions, iodide, and iodate, with spectroscopic techniques.

Chemometric analyses utilizing spectroscopic techniques have been successful in quantifying multiple analytes for monitoring nuclear material processing (Tse et al. 2020) and have been shown to determine stoichiometry in nitrate and sulfate systems based on subtle changes to the spectra (Tse et al. 2020; Gal et al. 1992). Development of chemometric models could identify redox reactions of interest for process monitoring, but a better understanding of neutron induced radiolysis would be needed to be useful in monitoring an aqueous homogeneous subcritical system. There appears to be no correlation between uranium species and iodine species that could allow for indirect on-line monitoring of the chemical behavior of iodine to support emission abatement.

5.0 References

Al-Kayssi, M. and R. Magee. 1963. The Determination of Periodate by Infrared Spectroscopy. Analytica Chimica Acta 28: 176-178.

Alvarez, L., J. Bantignies, R. Le Parc, R. Aznar, J. Sauvajol, A. Merlen, D. Machon, and A. San Miguel. 2010. High-Pressure Behavior of Polyiodides Confined into Single-Walled Carbon Nanotubes: A Raman Study. Physical Review B: Condensed Matter and Materials Physics (1998-2015), American Physical Society, 82(20): 205403.

Arrigo, L.M., R.N. Christensen, C.G. Fraga, M. Liezers, S.M. Peper, E.M. Thomas, S.A. Bryan, M. Douglas, A.R. Laspe, A.M. Lines, J.M. Peterson, A.J. Casella, D.C. Duckworth, T.G. Levitskaia, C.R. Orton, and J.M. Schwantes. 2009. FY 2009 Progress: Process Monitoring Technology Demonstration at PNNL. PNNL-19136.

Bray, W. and H. Liebhafsky. 1931. Reactions Involving Hydrogen Peroxide, Iodine, and Iodate Ion. Journal of the American Chemical Society 51(1): 38-44.

Burneau, A. and M. Tazi. 1997. Raman Spectroscopic Determination of Equilibrium Constants of Uranyl Sulphate Complexes in Aqueous Solutions. Talanta, 39(7): 743-748.

Carter, J. S. 1925. CCCXCVI. – The Salting-out Effect. The Influence of Electrolytes on the Solubility of Iodine in Water. Journal of the Chemical Society. 127: 2861-2866

Choppin, G., J. Liljenzin, and J. Rydberg. 2002. Radiochemistry and Nuclear Chemistry. Woburn, MA. Butterworth-Heinemann.

Cook, P., P. Carpenter, and E. Butler. 2000. Speciation of Dissolved Iodine in the Waters of a Humic-Rich Estuary. Marine Chemistry 69(3-4): 179-192.

CRC Handbook of Chemistry and Physics, 2009-2010, 90th ed. Edited by D.R. Lide, and W.M. Haynes, Associate Editor (National Institute of Standards and Technology, Gaithersburg, MD, USA). CRC Press (an imprint of Taylor & Francis Group): Boca Raton, FL. 2009.

Crouthamel, C., H. Meek, D. Martin, and C. Banks. 1949. Spectrophotometric studies of Dilute Aqueous Periodate Solutions. Journal of the American Chemical Society 71(9): 3031-3035.

Dasent, W. and T. Waddington. 1960. Iodine-Oxygen Compounds. Part 1. Infrared Spectra and Structure of Iodates. Journal of the Chemical Society 2429-2432.

Elding, L. and L. Olsson. 1986. Stabilities, Solubility, and Kinetics and Mechanisms for Formation and Hydrolysis of some Palladium(II) and Platinum(II) Iodo Complexes in Aqueous Solution. Inorganica Chimica Acta 117(1): 9-16.

Gal, M., P.L. Goggin, and J. Mink. 1992. Vibrational spectroscopic studies of uranyl complexes in aqueous and non-aqueous solutions. Spectrochimica Acta, 48(1): 121-132.

Gardiner, D., R. Girling, and R. Hester. 1972. Vibrational Spectra and Force Constants of Chlorate, Bromate, and Iodate Ions in Aqueous Solution. Journal of Molecular Structure 13(1): 105-114.

Greenwood, N.N., and A. Earnshaw. 1997. “Chemistry of the Elements.” 2nd Edition. Elsevier Ltd. 1997

Iizuka, M., T. Inoue, O. Shirai, T. Iwai, and Y. Arai. 2001. Application of normal pulse voltammetry to on-line monitoring of actinide concentrations in molten salt electrolyte. Journal of Nuclear Materials 297(1): 43-51.

Jiang, P., Y. Katsumura, R. Nagaishi, M. Domae, K. Ishikawa, K. Ishigure, and Y. Yoshida. 1992. Pulse radiolysis study of concentrated sulfuric acid solutions. Formation mechanism, yield and reactivity of sulfate radicals. Journal of the Chemical Society, Faraday Transactions 88(12): 1653-1658.

Kaiho, T. 2015. Iodine Chemistry and Applications. New York, John Wiley& Sons, Inc.

Karbowiak, M., B. Fourest, S. Hubert, and C. Moulin. 2003. Complexation of U(VI) with Iodate Ions: Determination of Stability Constants by using Spectroscopic Methods and Capillary Zone Electrophoresis. Radiochimica Acta, 91(9): 505-512.

Keilholtz, G. and C. Barton. 1965. Behavior of Iodine in Reactor Containment Systems. Oak Ridge National Laboratory, Nuclear Safety Information Center.

Kireev, S. and S. Shnyrev. 2015. Study of Molecular Iodine, Iodate Ions, Iodide Ions, and Triiodide Ions Solutions Absorption in the UV and Visible Light Spectra Bands. Laser Physics 25: 075602.

Kirsanov, D., A. Rudnitskaya, and A. Legin. 2017. UV-Vis Spectroscopy with Chemometric Data Treatment: an Option for On-line Control in Nuclear Industry. Journal of Radioanalytical Nuclear Chemistry, 312: 461-470. DOI 10.1007/s10967-017-5252-8.

Lefèvre, G., A. Walcarius, J. Ehrhardt, and J. Bessière. 2000. Sorption of Iodide on Cuprite (Cu_2O). Langmuir 16(10): 4519-4527.

Leiterer, M., D. Truckenbrody, and K. Franke. 2001. Determination of Iodine Species in Milk using Ion Chromatographic Separation and ICP-MS Detection. European Food Research and Technology 213: 150-153.

Liebhafsky, H. 1931. Reactions Involving Hydrogen Peroxide, Iodine, and Iodate Ion. III. The Reduction of Iodate by Hydrogen Peroxide. Journal of the American Chemical Society 53(3): 896-911.

Liebhafsky, H. 1932. The Catalytic Decomposition of Hydrogen Peroxide by the Iodine-Iodide Couple. II and III. The Rate of Oxidation in Neutral, and in Acid, Solution of Hydrogen Peroxide by Iodine. Journal of the American Chemical Society 54: 3499-3508.

Liebhafsky, H. 1934. The Catalytic Decomposition of Hydrogen Peroxide by the Iodine-Iodide Couple. IV. The Approach to Steady State. Journal of the American Chemical Society 56: 2369-2372.

Liebhafsky, H., R. Furuichi, and G. Roe. 1981. Reactions Involving Hydrogen Peroxide, Iodine, and Iodate ion. 7. The Smooth Catalytic Decomposition of Hydrogen Peroxide, Mainly at 50°C. Journal of the American Chemical Society 103(1): 51-56.

Liebhafsky, H., W. McGavock, R. Reyes, G. Roe, and L. Wu. 1978. Reactions Involving Hydrogen Peroxide, iodine, and Iodate Ion. 6. Oxidation of Iodine by Hydrogen Peroxide at 50°C. Journal of the American Chemical Society 100(1): 87-91.

Liebhafsky, H. and L. Wu. 1974. Reactions Involving Hydrogen Peroxide, Iodine, and Iodate Ion. V. Introduction to the Oscillatory Decomposition of Hydrogen Peroxide. Journal of the American Chemical Society 96 (23): 7180-7187.

Lousada, C., I. Soroka, Y. Yagodzinskyy, N. Tarakina, O. Todoshchenko, H. Hänninen, P. Korzhavyi, and M. Jonsson. 2016. Gamma Radiation Induces Hydrogen Absorption by Copper in Water. Nature Scientific Reports 6: 24234.

Mincher, B., S. Mezyk, and L. Martin. 2008. A Pulse Radiolysis Investigation of the Reactions of Tributyl Phosphate with Radical Products of Aqueous Nitric Acid Irradiation. Journal of Physical Chemistry A 112(28): 6275-6280.

Mincher, B., G. Modolo, and S. Mezyk. 2009. Review Article: The Effects of Radiation Chemistry on Solvent Extraction: 1. Conditions in Acidic Solution and a review of TBP Radiolysis. Solvent Extraction and Ion Exchange 27: 1-25.

National Institute of Advanced Industrial Science and Technology. 2018. Spectral Database for Organic Compounds, SDBS. Accessed 9 9, 2021. https://sdbs.db.aist.go.jp/sdbs/cgi-bin/cre_index.cgi.

Nowak, M., and Z. Nowak. 1986. The Influence of Iodine on Radiolysis of PUREX-Solvent. Journal of Radioanalytical and Nuclear Chemistry Letters 103: 141-152.

Pearson, J., and Nilsson, M. 2014. Radiolysis of Tributyl Phosphate by Particles of High Linear Energy Transfer. Solvent Extraction and Ion Exchange 32: 584-600.

Pearson, R. 1963. Hard and Soft Acids and Bases. Journal of the American Chemical Society 85(22): 3533-3539.

Pienpinijtham, P., X. Han, S. Ekgasit, and Y. Ozaki. 2011. Highly Sensitive and Selective Determination of Iodide and Thiocyanate Concentrations Using Surface-Enhanced Raman Scattering of Starch-Reduced Gold Nanoparticles. Analytical Chemistry 83(10): 3655-3662.

Pourbaix, M. 1974. Atlas of Electrochemical Equilibria in Aqueous Solutions. Houston, TX. National Association of Corrosion Engineers.

Prins, G., E. Cordfunke, and W. Ouweltjes. 1978. Standard Enthalpies of Formation of Uranium Compounds V. UO2Br2, UO2Br2·H2O, UO2Br2·3H2O, and UO2(OH)Br·2H2O. A Comment on the Stability of Uranyl Iodide and its Hydrates. The Journal of Chemical Thermodynamics 10: 1003-1010.

Ragoussi, M-E., Martinez, J. S., Costa, D. 2020. Second Update on the Chemical Thermodynamics of Uranium, Neptunium, Plutonium, Americium, and Technetium. Boulogne-Billancourt (France). OECD Nuclear Energy Agency.

Sakurai, T., A. Takahashi, N. Ishikawa, and Y. Komaki. 1995. Interaction of Iodine with an Extractant of 30% TBP/70% n-Dodecane. Journal of Nuclear Science and Technology, 32(7): 664-670.

Sawai, T., Y. Shinozaki, and G. Meshitsuka. 1966. The Radiolysis of Aqueous Solutions of Potassium Iodide. Bulletin of the Chemical Society of Japan, 39(5): 951-955.

Semnami, A. and M. Shamsipur. 1996. Spectrophotometric Study of the Complexation of Iodine with Macrocycles in Chloroform Solution. Journal of the Chemical Society, Dalton Transactions 11: 2215-2218.

Shelor, C. and P. Dasgupta. 2011. Review of Analytical Methods for the Quantification of Iodine in Complex Matrices. Analytica Chimica Acta 702(1): 16-36.

Skoog, D., F. Holler, and T. Nieman. 1998. Principles of Instrumental Analysis. 5th Edition. Saunders College Publishing.

Srinivasan, T. and P. Vasudeva Rao. 2014. Red Oil Excursions: A Review. Separation Science and Technology 49(25) 2315-2329.

Svensson, P. and L. Kloo. 2003. Synthesis, Structure, and Bonding in Polyiodide and Metal Iodide - Iodide Systems. Chemical Reviews 103(5): 1649.

Tse, P., S. Bryan, N. Bessen, A. Lines, and J. Shafer. 2020. Review of on-line and near real-time spectroscopic monitoring of processes relevant to nuclear material management. Analytica Chimica Acta, 1107: 1-13. DOI 10.1016/j.aca.2020.02.008.

van Elteren, J., C. van den Berg, H. Zhang, T. Martin, and E. Achterberg, E. 1995. Automated In-Line Extraction of Uranium(VI) from Raffinate Streams with On-Line Detection by Cathodic Stripping Voltammetry. Analytical Chemistry 67(21): 3903-3910.

Van Stipdonk, M., V. Santiago, E. Schweikert, C. Chusuei, and D. Goodman, D. 2000. Secondary Ion Emission from keV Energy Atomic and Polyatomic Projectile Impacts on Sodium Iodate. International Journal of Mass Spectrometry 197(1-3): 149-161.

Wold, S. 1995. Chemometrics; What Do We Mean with It, and What Do We Want from It? Chemometrics and Intelligent Laboratory Systems 30: 109-115.

Wong, G. and L. Zhang. 1992. Determination of Total Inorganic Iodine in Seawater by Cathodic Stripping Square Wave Voltammetry. Talanta 39(4): 355-360.

Xu, L., G. Csekö, T. Kégl, and A. Horváth. 2012. General Pathway of Sulfur-Chain Breakage of Polythionates by Iodine Confirmed by the Kinetic and Mechanism of the Pentathionate-Iodine Reaction. Inorganic Chemistry 51: 7837-7843.

Yoshida, S., Y. Muramatsu, S. Katou, and H. Sekimoto. 2007. Determination of the Chemical forms of Iodine with IC-ICP-MS and its Application to Environmental Studies. Journal of Radioanalytical and Nuclear Chemistry 273(1): 211-214.

Zheng, J., M. Yamada, and S. Yoshida. 2011. Sensitive Iodine Speciation in Seawater by Multi-Mode Size-Exclusion Chromatography with Sector-Field ICP-MS. Journal of Analytical Atomic Spectrometry 26: 1790-1795.

Pacific Northwest National Laboratory

902 Battelle Boulevard
P.O. Box 999
Richland, WA 99354
1-888-375-PNNL (7665)

www.pnnl.gov